

UNCLASSIFIED

Defense Technical Information Center
Compilation Part Notice

ADP013669

TITLE: Hairpin Vortex Formation in Poiseuille Flow Due to Two-Hole Suction

DISTRIBUTION: Approved for public release, distribution unlimited

This paper is part of the following report:

TITLE: DNS/LES Progress and Challenges. Proceedings of the Third AFOSR International Conference on DNS/LES

To order the complete compilation report, use: ADA412801

The component part is provided here to allow users access to individually authored sections of proceedings, annals, symposia, etc. However, the component should be considered within the context of the overall compilation report and not as a stand-alone technical report.

The following component part numbers comprise the compilation report:

ADP013620 thru ADP013707

UNCLASSIFIED

HAIRPIN VORTEX FORMATION IN POISEUILLE FLOW DUE TO TWO-HOLE SUCTION

D. B. GOLDSTEIN

*Dept. of Aerospace Engineering and Engineering Mechanics
The University of Texas at Austin, Austin, TX 78712*

AND

J. COHEN AND V. LEVINSKI

*Faculty of Aerospace Engineering
Technion, Israel Institute of Technology, Haifa, Israel, 32000*

A virtual-surface DNS is used to examine hairpin formation caused by a pair of suction holes below a laminar wall-bounded flow. The work models an experiment, presently underway, in which quasi-periodic hairpins are to be generated in a laminar plane-Poiseuille flow. We present some brief preliminary studies of vortex dynamics and find both symmetric and antisymmetric modes of shedding. We also examine the effect of inter-hole spacing on hairpin formation.

1. Introduction

A turbulent boundary layer is known to consist mainly of two different kinds of coherent vortical structures: counter-rotating streamwise vortices observed in the near wall region and hairpin-shaped vortices extended across the boundary layer. The hairpin structure consists of a head reaching out into the log layer and long legs trailing behind and below in the buffer layer. There may be many variants on this model since a simple, isolated, symmetric hairpin can be hard to find in experimental or computational fully turbulent boundary layers. Assymmetric or one-legged structures are common and a visualization of a high Reynolds number simulation can often look like a confused mass of writhing worms. The hairpin structures extend from a near-wall region of high shear having more stream-aligned structures out into a much lower mean shear region. How each region influences the other remains open to discussion. There has also been much effort exerted in trying to fathom out how such coherent structures self-replicate. In a

turbulent boundary layer the hairpins may form as an instability along the low speed streaks. It is likely, however, is that there are several processes which occur with different frequencies and that if one looks closely, one process blends smoothly into another and becomes only distinguishable by degree.

Levinski and Cohen [6] (LC) proposed a new predictive theoretical model explaining the mechanism leading to the rapid growth of hairpin vortices in shear flows. Malkiel *et al* [7] provided further proof of this theory. LC focused on the evolution of localized disturbances (all dimensions of which are much smaller than the length scale corresponding to variations of the basic velocity shear) and used the fluid impulse integral to characterize this type of disturbance.

Their analysis showed that unidirectional planar shear flows are always unstable with respect to finite-amplitude localized disturbances. Furthermore, the analysis predicts that the initial vortex grows exponentially and that it is inclined at 45° to the basic flow direction. These predictions agree with existing experimental observations concerning the growth of hairpin vortices in laminar and turbulent boundary layers.

The resulting set of coupled equations obtained by Levinski and Cohen [6] describes the dynamics of the localized vorticity disturbance. Accordingly it is governed by two mechanisms: one is the lift-up of the disturbance in the cross-stream direction which stretches the basic spanwise vorticity field and thus generates a disturbance-vorticity component in the cross-stream direction; the other mechanism is associated with the stretching and rotation of this disturbed vortex by the basic shear field. This intensifies the streamwise vorticity component which, in turn, induces an increased cross-stream velocity, thereby enhancing the lift-up effect and closing the feedback loop. Once formed, the hairpin evolves through self-induction in the presence of the mean shear.

Computational modeling of the Couette flow hairpin device was done by Rosenfeld *et al* [9] who suggested hairpin formation due to a shedding of a vortical bridge between the holes. In an ongoing experiment, hairpins are to be generated in a laminar plane-Poiseuille flow by way of suction through a pair of small holes on one wall. Computations of the effect of similar distributed discrete suction holes by Meitz [8] examined how suction alters the stability of quiet flow, Klebanoff modes, and TS waves in a Blasius boundary layer. Meitz's work utilized a prescribed suction profile over the holes with forced spanwise symmetry and emphasized the effects of relatively lower suction levels than examined presently.

We here briefly examine the process through which such quasi-periodic hairpins can develop. There can be different modes of hairpin shedding with hairpins sometimes forming right between the suction holes, if the

flow has slight asymmetries, and at other times the hairpins roll up much further downstream. The suction holes obviously alter the mean (parabolic) flow field so whether the hairpins we examine correspond to those in an unperturbed flat plate boundary layer remains to be determined.

2. The Computational Approach

The present work uses an unconventional computational approach – solid surfaces are modeled by applying a body force to the flow to bring the flow to rest on a virtual surface. This approach for creating a virtual solid surface has been shown [1] to be sufficiently flexible and efficient to model laminar and turbulent flow over complicated geometries. That work also discusses the numerical stability of the method. Goldstein *et al* [2] provides a more detailed review of the virtual surface approach as well as grid resolution studies of laminar flow over riblets, an examination of the sensitivity of the solution to various smoothing parameters, and an in depth analysis of turbulent flow over virtual flat and textured plates. Goldstein and Tuan [3] produce exhaustive grid resolution studies showing convergence even in a turbulent flow over a ribbed surface using the same code as used herein.

The basis of the virtual surface model is that the surface being modeled is defined by a set of boundary points which exist within a region spanned by a fixed (Eulerian) mesh on which the flow equations are solved. The boundary points \mathbf{x}_s exert a body force on the fluid such that the flow comes to a desired velocity, \mathbf{U}_{des} , on \mathbf{x}_s . A key feature of the present approach is that flows around complex boundary geometries are reduced to ones which are fully rectilinear and hence are amenable to spectral methods (we use that of [5] and [4]). The virtual surface approach imposes only a small computational overhead and little in the way of a coding burden. Potential difficulties associated with the singular nature of the force field, addressed in Goldstein *et al* [1,2], are largely overcome by spatial smoothing and spectral filtering. The forcing function $\mathbf{f}(\mathbf{x}, t)$ is determined as $\mathbf{f}(\mathbf{x}, t) = \alpha \int_0^t \Delta \mathbf{U}(\mathbf{x}, t') dt' + \beta \Delta \mathbf{U}(\mathbf{x}, t)$ with $\Delta \mathbf{U} = \mathbf{U} - \mathbf{U}_{\text{des}}$ where the quantities α and β are negative constants (see [1]). On an immobile surface $\mathbf{U}_{\text{des}} = 0$. The lower surface is a virtual solid surface created with the force field (Fig. 1(a)). The flow is sucked into the holes in the surface due to the reduced pressure in the gap between the virtual surface and the ordinary flow field boundary. This low pressure is maintained by forced blowing ($\mathbf{U}_{\text{des}} = (0, v_{\text{blow}}, 0)$) out of a spanwise strip in the virtual surface well downstream of the suction holes.

A buffer zone, located immediately downstream of the blowing slot, is used to both maintain the parabolic velocity profile in the bulk of the domain and to absorb the perturbations introduced by the suction and blow-

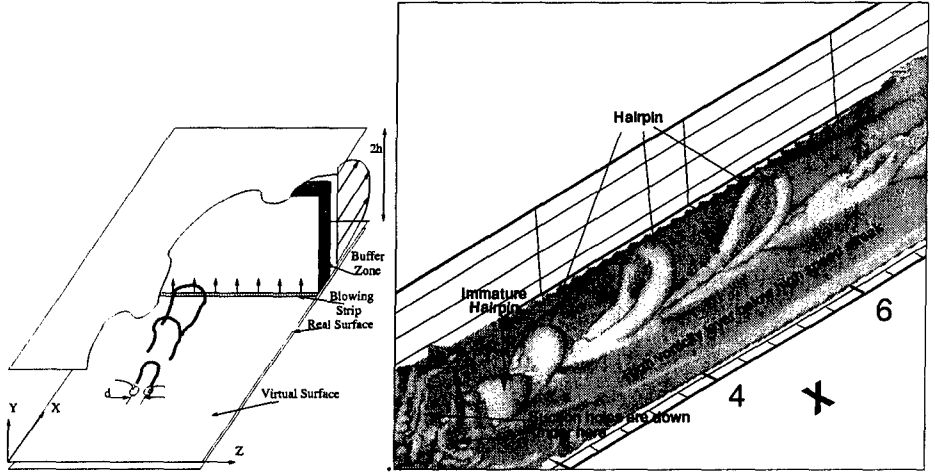


Figure 1. (a) Channel flow configuration for two-hole suction simulations. Channel is periodic in the streamwise (X) and spanwise directions (Z) and bounded by impermeable flat walls in the vertical direction (Y). Flow quantities are represented by Fourier expansions in the horizontal ($X-Z$) plane and a Chebyshev expansion in the wall normal direction. (b) Close-up of instantaneous isosurfaces of vorticity magnitude showing hairpins shedding in the wake of two holes. Flow from lower left.

ing sites. The buffer zone uses the force field to bring the flow to the desired parabolic profile. In order that this accommodation process be gradual, the quantities α and β are made to vary in the buffer region in a smooth manner as $\alpha_{buffer}(x) = 20e^{-120(\Delta i/W)^2}$ and $\beta_{buffer}(x) = 20e^{-12(\Delta i/W)^2}$ where W is the number of cells in the length of the buffer zone ($=25$) and Δi the number of cells distant from the center x -plane of the buffer region. The width of the α_{buffer} Gaussian is much narrower than that of the β_{buffer} Gaussian. α_{buffer} is a rather harsh term in that it makes the force adjust itself to completely cancel out the velocity error. This is of use in ensuring the steady mean flow. The β_{buffer} term surrounding the α_{buffer} core region damps nearly all of the temporal fluctuations before they reach the α_{buffer} layer. The present channel dimensions are chosen to be $12.9h:2h:6.46h$ in $x:y:z$ where h is the channel half-height and the grid is $128 \times 65 \times 128$.

3. Hairpin Formation

Figure 1(b) illustrates the nature of the hairpin vortices we obtain in our simulations. The channel Reynolds number based on centerline velocity, U_{cl} , and $h(=.9289)$, is 1115. The hole center-to-center spacing, d , is $0.84h$ and the holes are $7.32h$ upstream of the buffer layer. We give the volume flow rate through the holes, Q_{holes} by comparison to the volume which

would flow through the channel cross-sectional area bound by the top and bottom surfaces and the hole centerlines in the absence of suction: dhU_{mean} . That ratio is $dhU_{mean}/Q_{holes} = 5.86$. One incipient hairpin is forming just downstream of the holes and three others are seen further downstream in various stages of evolution. At this low Reynolds number the hairpins of figure 1(b) appear short and stocky. At higher Reynolds numbers the legs become longer and thinner and may develop a kink which evolves, through leg-to-leg reconnection, into two separate hairpins.

The holes continuously pull high speed fluid from well above the surface, down towards the surface. As a result, there is a continuous downflow of fluid both over the holes and in their wake. Figure 2(a), shows a close-up view of iso-vorticity contours in a ZY plane $2d$ downstream of the hole centerline. There is clearly a region of downwash just above each high (ω_z) vorticity streak in the wake of each hole. The head of a hairpin is just passing through the frame at this time.

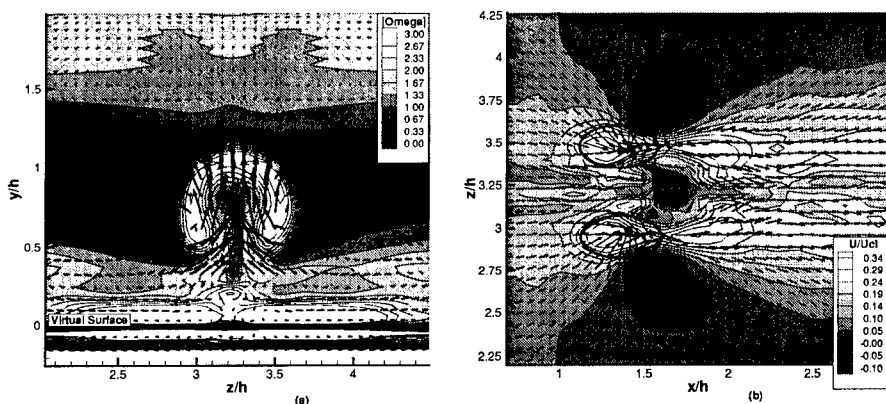


Figure 2. (a) Vorticity magnitude in a ZY plane showing slice of a hairpin head in the wake of two holes and (b) streamwise instantaneous velocity contours in a ZX plane near the suction holes (black ovals). Velocity vectors are also shown.

Figure 2(b) provides contours of the streamwise velocity U just above the virtual surface near the suction holes. It is clear that the holes draw in fluid nearly radially from the front and sides of the holes. The drawing down of high speed fluid from well above the surface creates a region of fluid just over the hole as well as just aft having a high U velocity. Moreover, the suction is strong enough to create a separated reverse flow region outboard of each hole.

We can interpret the flow in terms of the vorticity dynamics schematically shown in figure 3. The hairpins originate upstream of the holes. As

the near-wall spanwise vortex lines in the mean parabolic flow move downstream ahead of the holes, they are pulled into a downstream orientation by the suction thus rotating $-\omega_z$ vorticity into the x direction to create $\pm\omega_x$ vorticity. The vortex lines are strongly stretched, increasing in vorticity, as they are drawn down the holes. These stretched and rotated

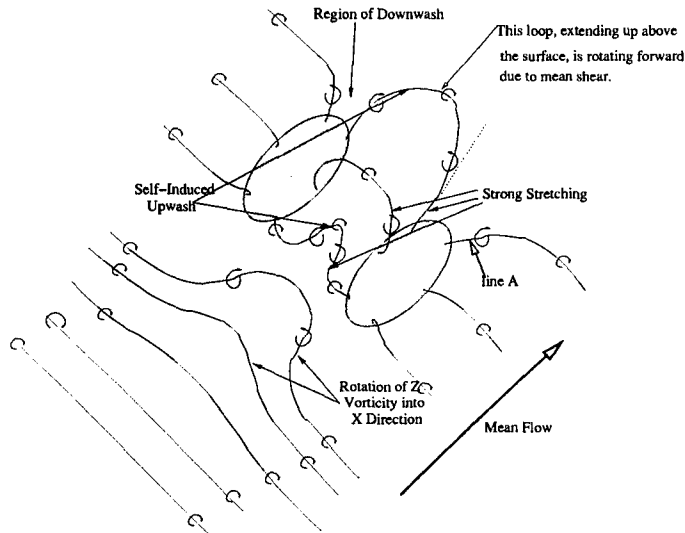


Figure 3. Close-up schematic of vortex line dynamics near suction holes. Note that this is meant to be a 3D perspective view and some of the lines project above the plane of the paper.

vortex lines produce a region of upwash along the centerline, upstream of the holes, that is surrounded by a pair of counter-rotating vortices of the same orientation as the hairpin legs downstream. Outboard of the holes the downward-dipping highly stretched spanwise vortex lines can produce the regions of reverse flow near the surface. The broken vortex lines drawn down a hole (e.g., line A) lead to a region of downwash behind the hole. That high-speed flow brought down toward the surface subsequently creates a persistent high ω_z vorticity streak in the wake of each hole. There is also a circumferential nest-like ring of high vorticity around each hole (not seen in these figures) caused by the high-speed flow drawn in over the hole rim.

So the looped vortex lines originate in the immediate vicinity of the holes, in a region of large pressure gradients and strong vortex line stretching. The upwash caused by these bent vortex lines between the holes brings low speed fluid away from the surface producing the central low speed

streak. How these vortex lines manage to roll into a thickened discrete hairpin appears to depend on flow symmetry. If the flow is symmetric across the central Z -normal plane between the holes, the central low speed streak and surrounding pair of streamwise vortices may extend a long distance downstream before the streak becomes unstable and sheds hairpins. Sometimes, however, we find that the low speed streak encounters a spanwise instability directly between the holes. When this occurs (fig. 4), the hairpins roll up and shed just aft of the holes. The shedding can switch between symmetric and asymmetric modes in an apparently random manner for some flow conditions but be locked into one mode for others.

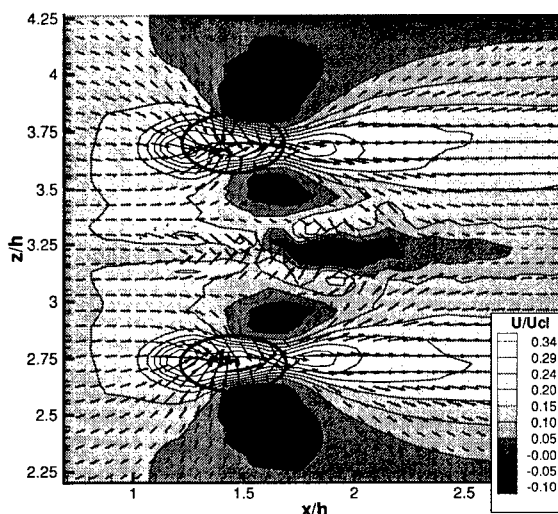


Figure 4. Instantaneous streamwise velocity contours and velocity vectors in a ZX plane near the suction holes. Note that the low speed streak between the holes is not symmetric but undergoes a flapping motion associated with hairpin roll-up immediately downstream of holes. In this case $d = .98h$, $Re = 3717$, and $dhU_{mean}/Q_{holes} = 6.80$

We ran a parametric study of the effect of hole spacing, d , on the nature of hairpin shedding by simply varying d while all other variables were kept constant (Reynolds number = 3717). Meitz [8], referencing Goldsmith (1957), utilizes a non-dimensional parameter for shear, $T = \frac{d^2}{2\nu} \frac{du}{dy}|_{wall} (\frac{d-D}{d})^{1.18}$ where $\frac{du}{dy}|_{wall}$ is the velocity gradient at the wall and D is the hole diameter, and a non-dimensional suction flux, $F = \frac{1}{\nu} \frac{Q_{holes}}{\Delta z} (\frac{d-D}{d})^{0.62}$ where $\frac{Q_{holes}}{\Delta z}$ is the suction flow volume per unit spanwise length. Both Meitz and Goldsmith examined circular uniformly spaced holes while our holes have an

aspect ratio of 2.7 and are nearly isolated pairs. Nonetheless, whether we choose D to be the hole width, hole length, or the geometric mean, our values of T are $O(10^1 - 10^3)$, within the range suggested by Meitz and Goldsmith to produce hairpin shedding if $F > \sim 37$. Yet we find shedding for lower values of F regardless of what D we choose or whether we take $\Delta z = d$ or equal to the domain width. Only for the smallest value of d ($d/h = 0.44$) do we find that the flow becomes steady. As we increase d , we first find low frequency shedding with the hairpins forming symmetrically, well downstream of the holes. For $d \sim 1$, asymmetric near-hole shedding also occurs.

Acknowledgment

The computations were performed at the University of Texas Center for High Performance Computing and were supported by AFOSR under grant F49620-98-1-0027 monitored by Dr. Thomas Beutner and through a Lady Davis Fellowship at the Technion.

References

1. D. Goldstein, R. Handler, and L. Sirovich, 1993a, "Modeling a no-slip flow boundary with an external force field," *J. Comp. Phys.* **105**, 354-366.
2. D. Goldstein, R. Handler, and L. Sirovich, 1995, "Direct numerical simulation of turbulent flow over a modelled riblet covered surface," *J. Fluid Mech.*, **302**, 333-376.
3. D. Goldstein and Tuan, T.-C., 1998, "Secondary flow induced by riblets," *J. Fluid Mech.*, **363**, 115-151.
4. R. A. Handler, E. W. Hendricks, and R. I. Leighton, 1989, Low Reynolds Number Calculation of Turbulent Channel Flow: A General Discussion. NRL Memorandum Report 6410, p. 1-103.
5. J. Kim, P. Moin, and R. Moser, 1987, "Turbulence statistics in fully developed channel flow at low Reynolds number," *J. Fluid Mech.*, **177**, 133.
6. V. Levinski and J. Cohen, 1995, "The evolution of a localized vortex disturbance in external shear flows. Part 1. Theoretical considerations and preliminary experimental results," *J. Fluid Mech.*, **289**, pp. 159-177.
7. E. Malkiel, V. Levinski and J. Cohen, 1999, "The evolution of a localized vortex disturbance in external shear flows. Part 2. Comparison with experiments in rotating shear flows," *J. Fluid Mech.*, **379**, pp. 351-380.
8. H. L. Meitz, 1996, *Numerical investigation of suction in a transitional flat-plate boundary layer*, PhD Dissertation, Univ. of Arizona.
9. M. Rosenfeld, J. Cohen and V. Levinski, 1999, "The evolution of hairpin vortices in rotating shear flows. Numerical Simulations," Proceedings of the 39th Israel Annual Conference on Aerospace Sciences, Israel, Feb. 17-18, pages: 11-19.